# Robotic Hand with Object-Manipulation and Emotion-Expression Capabilities

**Kyoung-Dae Kim, Yong K. Hwang, Won Sik Song, Manjai Lee**
Digital Media Laboratory, Information and Communications University, Seoul, Korea
*kdkim@icu.ac.kr, ykhwang@icu.ac.kr, songcode78@icu.ac.kr, manjai@icu.ac.kr*

**Abstract**

This paper presents a multi-fingered robotic hand called ICU Hand-I that we have developed with home-service robot applications in mind. Development of home-service robots are heavily funded in several countries in the world as it is perceived as the next big thing in the high-tech marketplace. Home-service robots are expected to function both as a servant and as a companion. The capability of manipulating common household items is important for robots to perform as servants, while emotion expression and interaction capability with humans are vital for robots to be companions to humans. Our hand is developed with these dual requirements in mind, striking the balance between dexterity, emotion expressing functions and the mechanical constraints of the fingers. The result is a hand with 4 fingers and a thumb driven by a tendon system, a total of 14 joints with 10 degrees of freedom and 4 passive linkages. Mathematically-rigorous inverse kinematics equations for passive linkages are developed during the hand design instead of using rule of a thumb. In addition, four kinds of emotion expressing functions are implemented: warming and cooling of the hand, vibration of the palm, pressure- controlled grasping and sweating of the palm. Although several sophisticated robotic hands have been developed that look like a human hand, we believe that our robotic hand is the first one that incorporates both manipulability and emotion-expression requirements.

**Key words**: robotic hand, emotion, interaction

## 1. Introduction

It is expected that home-service robots will be a one of the major household consumer items in the near future. There are several robotic vacuum cleaners in the market already [1, 2, 3] with affordable prices, and big companies are diligently investing in the development of robots that can do more household chores and be a companion to humans as well [4, 5, 6]. For a robot to be able to do typical household tasks, however, a lot more research is needed to bring up robots to industry standards. For home-service robots, humanoid robots are the most popular form because the human environment is built for the convenience of humans with the average physique. Many researchers in the world have been trying to build a useful humanoid robot [7, 8], and many technologies have been developed to varying degrees of success, such as artificial intelligence, mobility, object manipulation, human-robot interface and interaction. This paper concentrates on the robotic hand for home-service robots. The robotic hand is one of the major research topics in object manipulation category. When a robot tries to grasp or manipulate some objects in environment, the robot has to have high degrees of dexterity to complete the required task efficiently. Therefore, many researchers have built robotic hands that have high degrees of freedom (DOF) [9, 10, 12] to increase the manipulability. Besides the object manipulation problem, there is another issue for the robotic hand when a robot co-exists with humans. The robot inevitably has to interact with humans through voice and visual communication, but also with physical interactions especially with human hands and those of the robot. Physical interactions occur when a human gives or takes an object from a robot. In other cases, a human and a robot may shake hands, or touch each other to indicate emotional states or affection. If service robots are to perform both as a servant and companion, it is reasonable to assume that the robotic hand has to have a good dexterity for object manipulation, and capabilities to express emotions in some form. Our research has focused on balancing these two requirements for the robotic hand, and we believe it is the first of its kind to have such dual functionalities.

In this paper, we first present the mechanism design of a robotic hand system, named ICU Hand-I, and describe the kinematics and inverse-kinematics of ICU Hand-I in detail. Next, we define the functionalities for expressing emotions, and describe their hardware implementation in the robotic hand. The prototype is then tested for object grasping tasks as well as a human-interaction task, namely, handshaking. Finally, conclusions and future work are described in Section 5.

## 2. Design

The human hand is consisted of a thumb, four fingers and a palm. The thumb finger has three phalanxes and four DOFs in motion, while the other four fingers have four phalanxes including MP (Metacarpal Phalanx) and four DOFs. In each finger, MP (Metacarpal Phalanx) joint has two DOFs for flexion-extension and adduction-abduction movements.

The PIP (Proximal Interphalanx), MIP (Middle Interphalanx) and DIP (Distal Interphalanx) have only the flexion-extension movement [11] (see Figure 1).

Many researchers have constructed robotic hands that have a comparable manipulability as the human hand, and have succeeded in various object manipulation tasks such as manipulation in space or high-speed catching [9, 13].

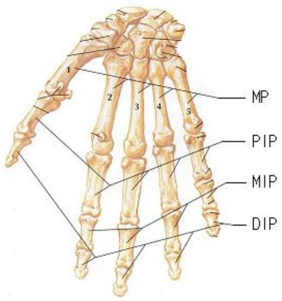


Fig. 1 Bones of a human hand

## 2.1. Mechanism Design

The design focus of our robotic hand is both object manipulation and human interaction. We tried to design it to have the similar shape and size of the human hand and to have basic grasping functionalities like cylindrical grasp, tip and hook [11]. The finger mechanism of ICU Hand-I includes only the flexion-extension for mechanism simplicity, although abduction-adduction is an important movement when the hand attempts in-hand manipulation of an object. Inclusion of abduction-adduction would adversely affect the shape, size and mechanism simplicity. Another important fact is that the human hand's DIP (Distal Interphalanx) joint does not necessarily have a separate actuator. In most cases, DIP joint moves passively and rarely does an active motion. Therefore, we decided to make the DIP joint passive.

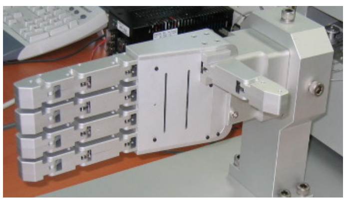

Fig. 2 ICU Hand-I

Figure 2 shows ICU Hand-I that we have developed –it has four fingers and a thumb and has 10 DOFs in total. Each finger has two independently controllable joints and one passive DIP joint. But, the thumb has two independently controllable joints without a passive joint. All joints of the hand are actuated by tendons like the hands in [14], and all tendons are controlled by DC servo motors to make joint motion.

As shown in Figure 3, the flexion motion is generated when the applied tendon force F is increased and extension motion is automatically generated by the restitutive force of the spring when the tendon force is decreased. We used a inter-connected link to generate the passive DIP joint motion that is determined by the MIP joint motion.

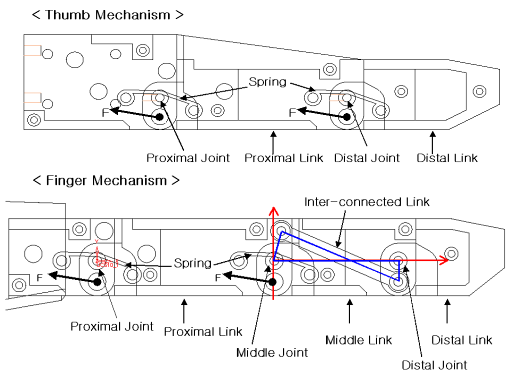


Fig. 3 Finger Mechanism

## 2.2. Forward-Kinematics Analysis

As stated above, we designed the distal joint of finger to do a passive motion according to the middle joint motion. The DIP joint motion is induced as the relative joint angle between the PIP and MIP increases. The passive-joint mechanism can be considered and analyzed as a four-bar linkage system.

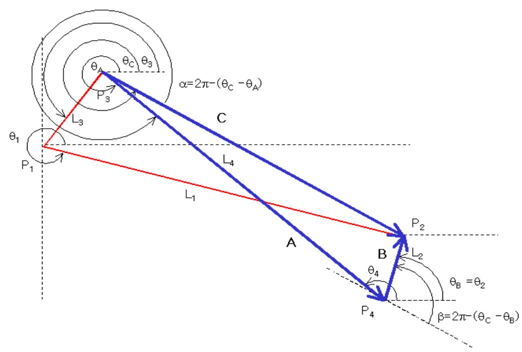


Fig. 4 Four-bar Linkage System

Figure 4. shows the kinematical configuration of the four-bar linkage system. The $\theta_1$ represents the MIP joint angle and $\theta_2$ represents the DIP joint angle in addition to its initial value $\theta_2(0)$.

From the complex polar algebra, we can derive the kinematic relationship between the MIP joint motion and the passive DIP joint motion as follows [15].

$$C = \sqrt{L_1^2 + L_3^2 + 2L_1L_3\cos(\theta_3 - \theta_1)} \tag{1}$$

$$\theta_C = \tan^{-1}\left(\frac{L_1\sin\theta_1 + L_3\sin\theta_3}{L_1\cos\theta_1 + L_3\cos\theta_3}\right) \tag{2}$$

From (1) and (2), the $\theta_2$ and $\theta_4$ are derived as follows.

$$\theta_2 = \theta_C \pm \cos^{-1}\left(\frac{C^2 + L_2^2 - L_4^2}{2CL_2}\right) \tag{3}$$

$$\theta_4 = \theta_C \mp \cos^{-1}\left(\frac{C^2 + L_4^2 - L_2^2}{2CL_4}\right) \tag{4}$$

$$\theta_3 = const \tag{5}$$

The angular velocities of Link 2($L_2$) and Link 4($L_4$) can be obtained from the vector relationship at Point 4($P_4$) as in Equation (6).

$$\dot{\vec{P}}_4 = \dot{\vec{L}}_1 + \dot{\vec{L}}_2 = \dot{\vec{L}}_3 + \dot{\vec{L}}_4 \tag{6}$$

$$\begin{Bmatrix} \dot{\theta}_2 \\ \dot{\theta}_4 \end{Bmatrix} = \begin{bmatrix} L_2 \cos\theta_2 & -L_4 \cos\theta_4 \\ L_2 \sin\theta_2 & -L_4 \sin\theta_4 \end{bmatrix}^{-1} \begin{Bmatrix} -(L_1 \cos\theta_1)\dot{\theta}_1 \\ -(L_1 \sin\theta_1)\dot{\theta}_1 \end{Bmatrix} \tag{7}$$

Equation (7) is the angular velocity relationship between the input angular velocity of $\theta_1$ and the output angular velocity of $\theta_2$ and $\theta_4$. From this equation, we can see that there is a singular condition when Link 4($L_4$) and Link 2($L_2$) are aligned in the same direction. Equation (8) describes the conditions in which this singularity occurs.

$$\theta_2 = \theta_4 \pm n\pi \qquad (n = 0, 1, 2, \cdots) \tag{8}$$

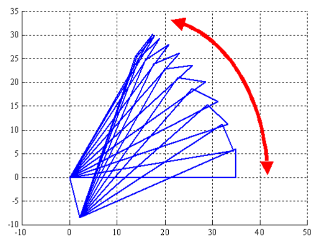

Fig. 5 Motion of Four-bar Linkage System

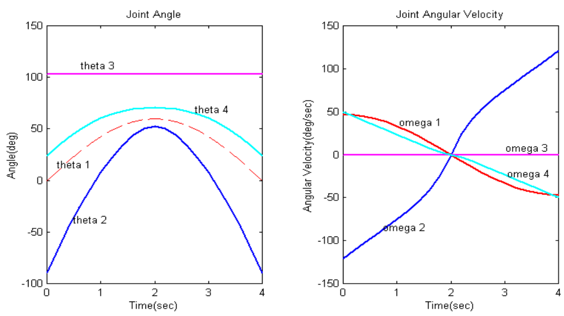


Fig. 6 Four-bar Linkage System Simulation

The motion analysis of the four-bar linkage system is verified with the simulation as shown in Figure 5 and 6. In this simulation, $\theta_1$ is the input and the outputs are $\theta_2$ and $\theta_4$.

All the coordinate systems of the hand are defined as in Figure 7. Because the thumb and the fingers have only the flexion-extension mobility, there is no motion in Z direction. We therefore define the coordinate system as a planar one, and the detailed dimensions of ICU Hand-I

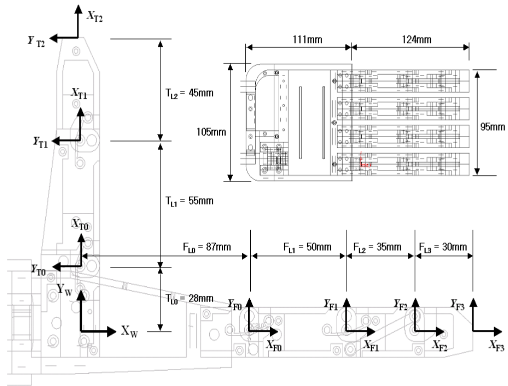


Fig. 7 Hand Dimension and Coordinate System

are also specified in Figure 7.

$$X_{ThumbTip} = T_{L0} \sin\theta_{T0} + T_{L1} \sin(\theta_{T0} + \theta_{T1}) + T_{L2} \sin(\theta_{T0} + \theta_{T1} + \theta_{T2}) \tag{9}$$

$$Y_{ThumbTip} = T_{L0} \cos\theta_{T0} + T_{L1} \cos(\theta_{T0} + \theta_{T1}) + T_{L2} \cos(\theta_{T0} + \theta_{T1} + \theta_{T2}) \tag{10}$$

$$X_{FingerbTip} = F_{L0} \cos\theta_{F0} + F_{L1} \cos(\theta_{F0} + \theta_{F1}) + F_{L2} \cos(\theta_{F0} + \theta_{F1} + \theta_{F2}) + F_{L3} \cos(\theta_{F0} + \theta_{F1} + \theta_{F2} + \theta_{F3}) \tag{11}$$

$$Y_{FingerbTip} = F_{L0} \sin\theta_{F0} + F_{L1} \sin(\theta_{F0} + \theta_{F1}) + F_{L2} \sin(\theta_{F0} + \theta_{F1} + \theta_{F2}) + F_{L3} \sin(\theta_{F0} + \theta_{F1} + \theta_{F2} + \theta_{F3}) \tag{12}$$

Equation (9), (10) are the forward kinematics of the thumb and Equation (11), (12) are the forward kinematics of the four fingers, which are derived from Figure 7. In these equations, $\theta_{T0}$ and $\theta_{F0}$ are constants and their values are 90(deg) and 0(deg), respectively. The following figures show the simulation result of this forward kinematics. Please note that the DIP joint moves passively almost at twice the speed of the MIP joint motion.

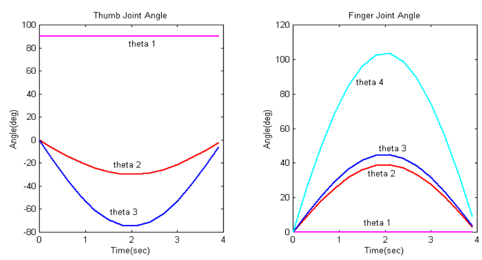


Fig. 8 Joint Angle Input for Hand Motion

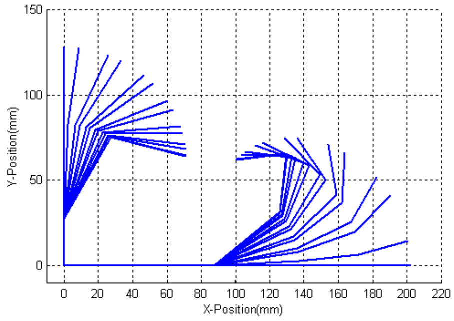


Fig. 9 Hand Motion by Forward Kinematics

### 2.3 Inverse-Kinematics Analysis

The inverse kinematics of the thumb can be derived from the derivative of the forward kinematics equations.

$$\begin{Bmatrix} \dot{\theta}_{T1} \\ \dot{\theta}_{T2} \end{Bmatrix} = \begin{bmatrix} a_{11} & a_{12} \\ a_{21} & a_{22} \end{bmatrix}^{-1} \begin{Bmatrix} \dot{X}_{ThumbTip} \\ \dot{Y}_{ThumbTip} \end{Bmatrix} \tag{13}$$

$$\begin{aligned} a_{11} &= T_{L1}\cos(\theta_{T0}+\theta_{T1}) + T_{L2}\cos(\theta_{T0}+\theta_{T1}+\theta_{T2}) \\ a_{12} &= T_{L2}\cos(\theta_{T0}+\theta_{T1}+\theta_{T2}) \\ a_{21} &= -T_{L1}\sin(\theta_{T0}+\theta_{T1}) - T_{L2}\sin(\theta_{T0}+\theta_{T1}+\theta_{T2}) \\ a_{22} &= -T_{L2}\sin(\theta_{T0}+\theta_{T1}+\theta_{T2}) \end{aligned}$$

As for the thumb, the velocity equations of the four fingers can be derived from the derivatives of Equation (11) and (12).

Equation (14) represents the relationship between the linear and angular velocities of four fingers when all joints are independently controllable. Equation (14), however, is not the exact form of the velocity equation of the four fingers because it does not consider the passive motion of DIP joint that is dependent on the motion of MIP joint. This equation can not be used to get the exact joint angular velocity from the linear velocity trajectory of the finger tip motion. Therefore, we have to reformulate this equation into a new one that includes the passive joint motion. To do this, we use the result of the four-bar linkage system analysis.

$$\begin{Bmatrix} \dot{X}_{FingerTip} \\ \dot{Y}_{FingerTip} \end{Bmatrix} = \begin{bmatrix} a_{11} & a_{12} & a_{13} \\ a_{21} & a_{22} & a_{23} \end{bmatrix} \begin{Bmatrix} \dot{\theta}_{F1} \\ \dot{\theta}_{F2} \\ \dot{\theta}_{F3} \end{Bmatrix} \tag{14}$$

$$\begin{aligned} a_{11} &= -F_{L1}\sin(\theta_{F0}+\theta_{F1}) + a_{12} \\ a_{12} &= -F_{L2}\sin(\theta_{F0}+\theta_{F1}+\theta_{F2}) + a_{13} \\ a_{13} &= -F_{L3}\sin(\theta_{F0}+\theta_{F1}+\theta_{F2}+\theta_{F3}) \\ a_{21} &= F_{L1}\cos(\theta_{F0}+\theta_{F1}) + a_{22} \\ a_{22} &= F_{L2}\cos(\theta_{F0}+\theta_{F1}+\theta_{F2}) + a_{23} \\ a_{23} &= F_{L3}\cos(\theta_{F0}+\theta_{F1}+\theta_{F2}+\theta_{F3}) \end{aligned}$$

$$\dot{\theta}_{F3} = \frac{L_1\sin(\theta_4-\theta_1)}{L_2\sin(\theta_2-\theta_4)}\dot{\theta}_{F2} \tag{15}$$

It is clear that $\theta_1$ is $\theta_{F2}$ and $\theta_2 + \theta_2\ (0)$ is $\theta_{F3}$ from Figure 3 and 4. And from Equation (7), we can get the relationship between $\theta_{F2}$ and $\theta_{F3}$.

Equation (15) represents the input and output motion relation of the four-bar linkage system, and this should be applied to Equation (14) to get the exact inverse-kinematics equation of the four fingers as follows.

$$\begin{Bmatrix} \dot{X}_{FingerTip} \\ \dot{Y}_{FingerTip} \end{Bmatrix} = \begin{bmatrix} a_{11} & \hat{a}_{12} \\ a_{21} & \hat{a}_{22} \end{bmatrix} \begin{Bmatrix} \dot{\theta}_{F1} \\ \dot{\theta}_{F2} \end{Bmatrix} \tag{16}$$

$$\hat{a}_{12} = \left( a_{12} + a_{13}\frac{L_1\sin(\theta_4-\theta_1)}{L_2\sin(\theta_2-\theta_4)} \right)$$

$$\hat{a}_{22} = \left( a_{22} + a_{23}\frac{L_1\sin(\theta_4-\theta_1)}{L_2\sin(\theta_2-\theta_4)} \right)$$

$$\begin{Bmatrix} \dot{\theta}_{F1} \\ \dot{\theta}_{F2} \end{Bmatrix} = \begin{bmatrix} a_{11} & \hat{a}_{12} \\ a_{21} & \hat{a}_{22} \end{bmatrix}^{-1} \begin{Bmatrix} \dot{X}_{FingerTip} \\ \dot{Y}_{FingerTip} \end{Bmatrix} \tag{17}$$

Figure 10 and 11 show the simulation result of inverse-kinematics of the whole hand motion. The initial positions of the thumb and a finger are (32, 121) and (190, 42), respectively, while the desired target positions of the tips are (80, 80) and (90, 80), respectively. We use the linear path that connect the start and end positions of the tip motions for the inverse-kinematics computation.

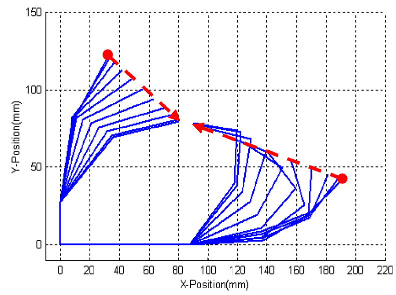


Fig. 10 Hand Motion by Inverse Kinematics

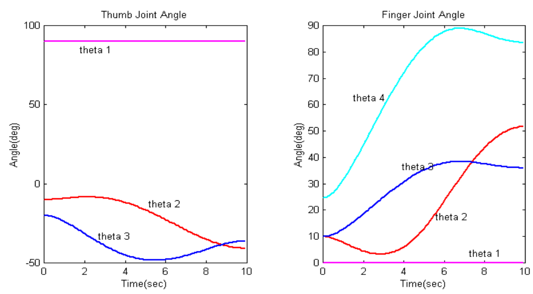


Fig. 11 Joint Angle by Inverse Kinematics

## 3. Emotion Functionalities

Robots will play the role of a guide in buildings or a butler in home. If robots have the capability of emotional interaction, people living together with a robot may feel more comfortable and feel intimacy. This factor will be more valuable when the robot owner spends most of his/her time alone in home. There are already some commercial robots that can do very simple emotional interactions with humans especially elderly people living alone. The Human Robot Interaction (HRI) occurs in several forms; the interactions through voice and vision are obviously the key parts of HRI. They can be used to transmit emotions. The hand also can transmit emotional messages through physical contacts. If we look at the pattern of interaction among people, we find that there are certain types of physical interactions especially using hands. Handshaking, holding hands and patting on the back are prime examples. When people shake hands with other people, the participants usually feel physical properties of the other person's hand. From this information people can usually tell the other person's current physical and/or emotional states.

### 3.1. Physical Properties Affected by Emotions

In general, humans shiver their hands when they feel cold, are under the state of tension, or are seized with fear. And when humans are in a very nervous situation or in an abnormal circumstance, their hands are soaked with sweats. For example, we can imagine a situation where we meet someone who is very famous and shake hands with him/her. Perhaps, most people will sweat in their hands and tremble involuntarily. Definitely, this is an expression of one's internal emotional state. Another example is when people control their grasping force according to the object to hold. The grasping force level will be widely different when grasping a baby's hand from when grasping an adult man's hand. When we shake hands with a very close friend who we have not met for a long time, we grasp the friend's hand much more firmly than in a normal situation. So the grasping force is another measure of emotional states.

### 3.2. Hand Design for Emotion Expression

We have tried to implement as many physical properties of the robotic hand as possible that could be used for emotion expression, and have come up with four: skin temperature, trembling, sweating and grasping force. Trembling, sweating and grasping force of the hand are key methods to express one's emotions as stated above. The skin and its temperature are important for the comfort factor. You may feel insecure or intimidated if a big, cold and high-powered metallic hand tries to grab your hand or arm, making you reluctant to interact with it. The skin texture and its proper level of temperature are important to make people to feel safe and allow them to interact with robots in a more comfortable manner.

We have imitated the trembling effect by attaching a few vibrating motors inside the palm of ICU Hand-I. A sheet-type heating pad is also installed on the surface of the palm to keep the hand at the human's skin temperature to minimize the metallic feeling of the robotic hand. In addition, a heat-exchange pad is attached to the palm. Depending on the polarity of the electricity applied, one side of the pad heats up while the other side cools down. This pad can give additional warmth for excitement or a "cold" hand expressing negative emotions. For the sweating system we have imitated the real sweating effect of human skin. We have used the fuel injecting system of a radio-control airplane to supply into the hand alcohol, which has an excellent volatility characteristic. Finally, an array of Force Sensing Resistors (FSR) is used to detect the contact force when the hand grasps an object. The following figure shows the components that we have used in ICU Hand-I for emotion expression.

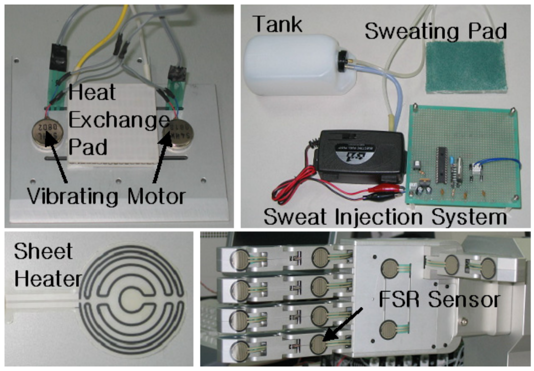


Fig. 12 Components for Emotion Expression of Robotic Hand

## 4. Experiment

### 4.1. System Configuration

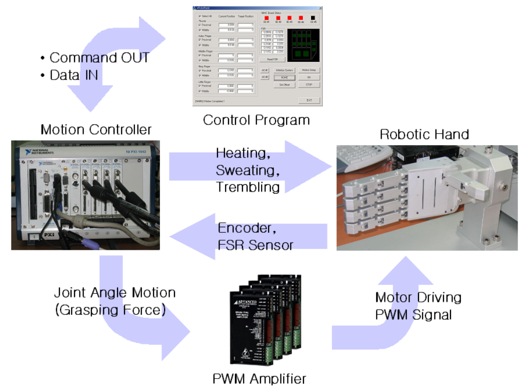


Fig. 13 System Configuration

The system consists of ICU Hand-I, a personal computer as the host computer, a PXI motion control system as the motor controller and a data interface system and a set of PWM amplifiers. The major actuator of ICU Hand-I system is a DC servo motor. We have used 10 motors to control all the active controllable joints.

The PXI control system controls the motors through analog signals which are converted and amplified to PWM signals to turn the DC-servo motors. Incremental encoders are used for position feedback, and the motion control is done every 500 microseconds using a PID control logic.

The skin is made of PVC(Polyvinyl Chloride) which is typically used for an artificial hand or arm. The material property is smooth and soft. A number of FSR sensors are attached evenly over the surfaces of fingers and the palm, and the sensed force data is collected through the PXI system's analog input channels.

### 4.2. Grasping Experiment

Because we have designed this robotic hand to have basic set of grasping modes such as cylindrical grasping, tip and hook, we have used various kinds of objects to see if the hand can make these types of gasping manipulation. Figure 14 shows some examples of object grasping.

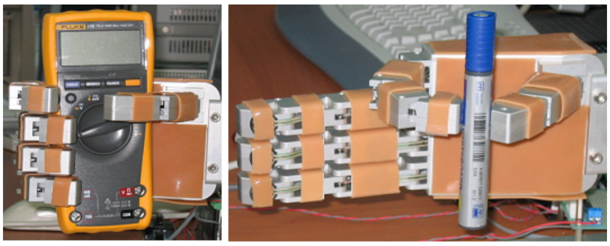

Fig. 14 Grasping Experiment with Various Types of Objects

### 4.3. Emotion Experiment

A number of people were asked to shake hands with the robotic hand with and without each of the emotion-expressing components. The results were close to what was expected and are shown in Table 1.

Table 1. People's reaction on handshaking with ICU Hand-1.

| Component | Off / Low /Cold | On/High/Hot |
|---|---|---|
| Overall skin temperature | indifferent, dead, boring, unresponsive | warm, friendly, comfortable |
| Chill /Hot pad | heartless, serious, mean | excited, angry |
| Vibration | calm, peaceful | excited, mild suspense |
| Grasping force | tender, passive | assertive, vigorous, fearful |
| Sweating | normal, clean | excited, unsanitary |

### 5. Conclusion

We have developed a robotic hand, ICU Hand-I, which has a similar shape and size of the human hand. ICU Hand-I has the basic object grasping capabilities, and can make several types of physical expressions by controlling grasping force, trembling, sweating, heating and chilling. We believe our hand is the first of its kind that has both object-manipulation capability and emotion-expression capability to the performance level presented in this paper.

In the future, we plan to improve the sensing capability of the robotic hand. If the robotic hand can sense the skin temperature, the resistor value of skin surface and other biological data of the interacting human, it can recognize human emotions and even provide healthcare services based on the obtained biological data.

### References


[1] Roomba Robotic Floorvac, http://www.roombavac.com

[2] Electrolux, http://www.robotbooks.com/robot-vacuum.htm

[3] Samsung,http://www.samsung.com/DigitAll/GlobalExhibition/Exhibition/ppk/VC_RP30W/ppk_VC_RP30W_m01.htm

[4] Asimo Special Site, http://www.honda.co.jp/ASIMO

[5] Qrio, http://www.sony.net/SonyInfo/QRIO

[6] Wakamaru,http://www.sdia.or.jp/mhikobe-e/products/etc/ robot.html

[7] Y.Sakagami, R.Watanabe, C.Aoyama, "The Intelligent ASIMO : System Overview and Integration", Proceedings of the 2002 IEEE/RSJ International Conference on Intelligent Robots and Systems, EPFL, Lausanne, Switzerland, 2002, pp. 2478-2483

[8] T. Ishida, Y. Kuroki, J. Yamaguchi, "Mechanical System of a Small Biped Entertainment Robot", Proceedings of the 2002 IEEE/RSJ International Conference on Intelligent Robots and Systems, Las Vegas, Nevada, 2003, pp. 1129-1134

[9] C.S. Lovchik, M.A.Diftler, "The Robonaut Hand : A Dexterous Robot Hand for Space", Proceedings of the 1999 IEEE International Conference on Robotics & Automation, Detroit, Michigan, 1999, pp. 907-912

[10] J.Butterfass, G.Hirzinger, S.Knoch, H.Liu, "DLR's multisensory articulated hand. I. Hard- and software architecture", Proceedings of the 1998 IEEE International Conference on Robotics & Automation, Leuven, Belgium, 1998, pp. 2081 – 2086

[11] N.Fukaya, S.Toyama, T.Asfour, R.Dillmann, "Design of the TUAT/Karlsruhe humanoid hand", Proceedings of the 2000 IEEE/RSJ International Conference on Intelligent Robots and Systems, Takamatsu, Japan, 2000, pp. 1754 – 1759

[12] L.R.Lin, H.P.Huang, "Integrating Fuzzy Control of the Dexterous National Taiwan University (NTU) Hand", IEEE/ASME Transactions on Mechatronics, vol.1, No.3, Sept., 1996

[13] A.Namiki, Y.Imai, M.Ishikawa, M.Kaneko, "Development of a High-speed Multifingered Hand System and Its Application to Catching", Proceedings of the 2003 IEEE/RSJ International Conference on Intelligent Robots and Systems, Las Vegas, Nevada, 2003, pp. 2666-2671

[14] Y.Ogahara, Y.Kawato, K.Takemura, T.Maeno, "A Wire-Driven Miniature Five Fingered Robot Hand using Elastic Elements as Joints", Proceedings of the 2003 IEEE/RSJ International Conference on Intelligent Robots and Systems, Las Vegas, Nevada, 2003, pp. 2672-2677

[15] J.E.Shigley, J.J.Uicker,Jr, "Theory of Machines and Mechanisms, 2nd edtition", McGraw-Hill, 1995